



Article

Enhancement of Luminescence Efficiency of Y_2O_3 Nanophosphor via Core/Shell Structure

Jae-Young Hyun ¹, Ki-Hyun Kim ², Jae-Pil Kim ², Won-Bin Im ³, Kadathala Linganna ^{2,*} and Ju-Hyeon Choi ^{2,*}

- ¹ Korea Conformity Laboratories, 17-22, Cheomdangwagi-ro 208 beon-gil, Buk-gu, Gwangju 61011, Korea; jyhyun@kcl.re.kr
- ² Intelligent Optical Module Research Center, Korea Photonics Technology Institute, Cheomdanventure-ro 108 beon-gil 9, Buk-gu, Gwangju 500-779, Korea; kimkh@kopti.re.kr (K.-H.K.); jpkim@kopti.re.kr (J.-P.K.)
- ³ Department of Materials Science and Engineering, Hanyang University, 222, Wangsimni-ro, Seongdong-gu, Seoul 04763, Korea; imwonbin@hanyang.ac.kr
- * Correspondence: lingannasvu@gmail.com (K.L.); juchoi2@kopti.re.kr (J.-H.C.); Tel.: +82-62-605-9562 (J.-H. C.)

Abstract: We successfully fabricated $Y_2O_3:RE^{3+}$ (RE = Eu, Tb, and Dy) core and core-shell nanophosphors by the molten salt method and sol-gel processes with Y_2O_3 core size of the order of 100~150 nm. The structural and morphological studies of the RE^{3+} -doped Y_2O_3 nanophosphors are analyzed by using XRD, SEM and TEM techniques, respectively. The concentration and annealing temperature dependent structural and luminescence characteristics were studied for $Y_2O_3:RE^{3+}$ core and core-shell nanophosphors. It is observed that the XRD peaks became narrower as annealing temperature increased in the core-shell nanophosphor. This indicates that annealing at higher temperature improves the crystallinity which in turn enhances the average crystallite size. The emission intensity and quantum yield of the Eu^{3+} -doped Y_2O_3 core and core-shell nanoparticles increased significantly when annealing temperature is varied from 450 to 550 °C. No considerable variation was noticed in the case of $Y_2O_3:Tb^{3+}$ and $Y_2O_3:Dy^{3+}$ core and core-shell nanophosphors.

Keywords: Y_2O_3 nanophosphor; core-shell structure; RE ions; luminescence efficiency; quantum yield



Citation: Hyun, J.-Y.; Kim, K.-H.; Kim, J.-P.; Im, W.-B.; Linganna, K.; Choi, J.-H. Enhancement of Luminescence Efficiency of Y_2O_3 Nanophosphor via Core/Shell Structure. *Nanomaterials* **2021**, *11*, 1563. <https://doi.org/10.3390/nano11061563>

Academic Editors: Wojciech Pisarski and Francisco Javier García Ruiz

Received: 30 April 2021
Accepted: 10 June 2021
Published: 14 June 2021

Publisher's Note: MDPI stays neutral with regard to jurisdictional claims in published maps and institutional affiliations.



Copyright: © 2021 by the authors. Licensee MDPI, Basel, Switzerland. This article is an open access article distributed under the terms and conditions of the Creative Commons Attribution (CC BY) license (<https://creativecommons.org/licenses/by/4.0/>).

1. Introduction

For the past few decades, nanomaterials have received particular attention for luminescence and photonic device application due to their interesting characteristics including high surface-to-volume ratio and the quantum confinement effect. When compared to bulk materials, these nanosized phosphors exhibit considerable modifications in the structure that include size, morphology, and crystallinity. Thus, in particular, rare earth-doped luminescent nanomaterials have been paid much attention as they play an important role in the luminescent devices such as displays, light emitting diodes, biological assays, and optoelectronics [1–4]. Rare-earth ions in a nanoscale host material are particularly interesting because of their unique properties such as luminescence in all spectral ranges from UV to IR, narrow emission linewidths, longer lifetime, and high quantum efficiency. Of the different sesquioxides, yttrium oxide (Y_2O_3) has been studied widely as a host material for rare earth ion doping in photonics and optoelectronics because of its thermo-mechanical properties, optical transparency (0.2–8 μm), and thermodynamically stable crystal structures. In addition, Y_2O_3 has a relatively low annealing temperature (400 °C), high refractive index (~1.8), and low maximum phonon energy (380 cm^{-1}), which make it a very promising host material for the production of efficient luminescent media, as well as for infrared ceramics [5]. Moreover, Y_2O_3 can be doped with different types of RE ions to produce strong luminescence over a wide range of wavelengths due to similarities in the atomic radii, crystal structure, and lattice constant of rare earth ions [6,7]. Among the rare earth ions, the Eu^{3+} , Tb^{3+} and Dy^{3+} are particularly interesting for display device

applications as they emit the luminescence in the visible region of red, green, and blue arising from the 4f–4f transitions, respectively.

In order to enhance the luminescence efficiency, it is necessary to control the phosphor size and crystallinity. In view of the above importance, numerous studies have been focused on different methods to synthesize nanocrystalline phosphor particles with different size and morphology, such as solid state reaction, spray pyrolysis, co-precipitation, sol–gel, solution combustion, hydrothermal, etc. Of the wet chemical methods, the molten salt synthesis technique has been used to produce single-phase nanoparticles at low processing temperature with a short duration reaction time and less residual filths. It is found that the rare earth-doped phosphors have shown a decrease in luminescence as the size of these particles changes to the nanoscale from the microscale due to the presence of parasitic surface quenching sites or partial diffusion of rare earth ions in host lattices, high rare earth dopant concentrations, and energy transfer to adjacent ions, that can quench the luminescence of rare earth ions in nanoparticles [8].

Therefore, it has been demonstrated that the passive shell layer around the core can reduce the surface OH^- groups' absorption and undesirable energy transfer between dopant ions, resulting increase in the luminescence properties [9,10]. The structure of the RE-doped active core as shown in the schematic diagram (see Figure 1a). As can be seen from Figure 1a, the optically active core directly interacts with the surface hydroxyl groups that can quench the luminescence intensity and lifetime of active core. A.K. Parchur et al. [9] and Dorman et al. [10] reported that the effect of the surface hydroxyl groups could be controlled by developing a passive shell layer around the core. The passive shell coated RE-doped active core is shown in the schematic diagram (Figure 1b). The core–shell nanostructures are used to increase the luminescence efficiency by removing the surface quenching sites. The purpose of the passive shell is to increase the distance between the surface quenching site and the doped ions in the core.

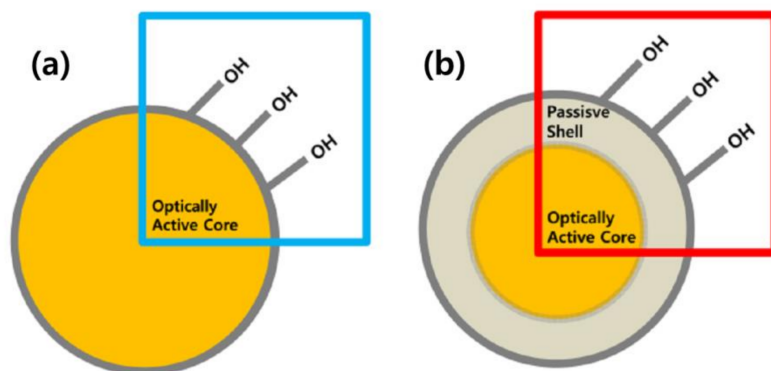


Figure 1. Schematic diagram of the structure of RE-doped (a) active core and (b) active core@passive shell.

Thus, in the present work, RE^{3+} (Eu, Tb, Dy)-doped Y_2O_3 nanophosphors with passive shells were fabricated by the molten synthesis method and sol–gel processes and their structural, morphological and luminescence properties studied with core–shell modification for the enhancement of luminescence efficiency.

2. Materials and Methods

2.1. Fabricated RE-Doped Y_2O_3 Core by the Molten Salt Method

The RE (Eu, Tb and Dy)-doped Y_2O_3 core nanoparticles were synthesized by molten salt synthesis using analytical grade $\text{Y}(\text{NO}_3)_3$ and $\text{RE}(\text{NO}_3)_3$ raw materials with purity of 99.9%. The RE-doped Y_2O_3 core nanoparticles were prepared according to the formula $(\text{Y}_{100-x}\text{RE}_x)_2\text{O}_3$ ($x = 0.05, 0.10, 0.15, 0.20$ for Eu, Tb and Dy). In the molten salt synthesis process, the RE raw materials were mixed with a 1.7:1 mole ratio of NaNO_3 and KNO_3 for 10 min, forming a well-mixed powder. Then, the mixture was taken into a covered

alumina crucible and heated in an electrical furnace at different temperatures of 450, 500, and 550 °C for 3 h. Then, the powders were cooled down to room temperature. The obtained powder was washed with deionized water until the salt solution was dilute enough to avoid crystallization of the supernatant. The remaining powders were dried at 100 °C overnight.

2.2. Y_2O_3 Passive Shell Coated Core

Deposition of the RE_2O_3 was carried out with the creation of a solution containing 5 mM urea (Sigma Aldrich, Seoul, Korea) and 0.1 mM $RECl_3$ (Alfa Aesar 99.9%, Incheon, Korea), depending on the desired thickness. The thickness of the shell layer was controlled by varying the ratio (χ) between the mass of the $RECl_3$ precursor and the mass of Y_2O_3 core particles. After the urea and RE salts were dissolved, 0.1 g of the Y_2O_3 was suspended in the solution and the liquid was sonicated for 30 min, to break apart agglomerates for complete mixing. The solution was heated at 80 °C for 4 h to promote the shell deposition. The resulting suspension was centrifuged and the resulting supernatant solutions were discarded. Afterwards, the particles were dried at 100 °C overnight. Finally, the powder was annealed at 750 °C for 3 h to remove any urea and to crystallize the RE_2O_3 shell.

2.3. Characterization Techniques

The structural analysis of RE-doped Y_2O_3 core nanophosphors was carried out using an X-ray diffractometer (PANalytical, Almelo, Netherlands) with Cu $K\alpha$ radiation ($\lambda = 1.54 \text{ \AA}$) as the source in the range of 10° to 80° at a step rate of 0.2°/min for crystalline phase identification. The passive shell layer structure was not analyzed using the XRD technique because of its low sensitivity as well as diffractions peaks overlapping in the range of 0° to 60°. The scanning electron microscope (SEM, Hitachi, S-4700, Houghton, Michigan, USA) was used for the identification of size of the synthesized RE-doped Y_2O_3 core and the Y_2O_3 passive shell coating thickness was confirmed using a transmission electron microscope (TEM, FEI TECNAL, F20UT, Hillsboro, OR, USA). The luminescence spectra were measured for the RE-doped core and core-shell nanoparticles using a spectrofluorimeter (Horiba Jobin Yvon Fluorolog3, Irvine, CA, USA). The quantum yield measurements were carried out using an absolute photoluminescence quantum yields measurement system (Horiba Jobin Yvon Fluorolog3, Irvine, CA, USA).

3. Results and Discussion

Figure 2a–c show the diffraction patterns of the as-prepared and RE^{3+} -doped Y_2O_3 nanophosphors annealed at different temperatures and were obtained by X-ray diffractometer under the same experimental conditions. The XRD spectra showed a distinctive peaks and clearly indicate crystalline nature even for the as-prepared Y_2O_3 sample. The observed diffraction peaks are indexed to (211), (222), (400), (440), and (622) of cubic Y_2O_3 and matched to the JCPDS card no. 41–1105. This indicated that the as-prepared and RE^{3+} -doped nanoparticles have the characteristic Y_2O_3 cubic structure with space group of $Ia\bar{3}$. A strong peak at $2\theta = 29.5^\circ$ was observed, attributed to the plane (222). Similar behavior has been reported elsewhere [11–15]. An annealing process was performed for the RE^{3+} -doped nanophosphors in order to disperse the RE ions into the lattice and in turn to increase the total luminescence of the nanoparticles. The samples were annealed in the range from 450 to 550 °C for 3 h. The position of the diffraction peaks was not changed with the applied annealing temperature and confirm the presence of single cubic crystalline structure of RE-doped Y_2O_3 nanoparticles. Figure 2d depicts the variation of peak width (FWHM) as a function of annealing temperature varied from 450 to 550 °C in RE^{3+} -doped Y_2O_3 nanophosphors. It can be observed that the XRD peaks become narrower on annealing the samples at higher temperatures. Based on the narrowing of the diffraction peaks, it can be concluded that the size of the crystallites increases. An indication of crystallinity increase could be flattening of the amorphous hump (if present) or possibly lowering of

the baseline. The crystallite size (D) of RE^{3+} -doped nanophosphors can be estimated from the well-known Debye–Scherrer’s equation shown below [16],

$$D = \frac{0.9\lambda}{\beta \cos \theta}$$

where λ is the wavelength of the X-ray source (1.5406 Å), β is the full width at half maximum of intense diffraction peak (222) in the XRD pattern, and θ is the Bragg diffraction angle. The crystallite size of the RE^{3+} -doped nanophosphors annealed at different temperatures was calculated using the Scherrer’s equation and tabulated in Table 1. It was noted that the crystallite size of the nanophosphors increased as the annealing temperature increased from 450 °C to 550 °C. The crystallite size of the present nanophosphors calculated from the Scherrer’s equation was compared to the crystallite size of the RE^{3+} -doped nanophosphors determined from the Hall–Williamsons equation as shown in Table 1.

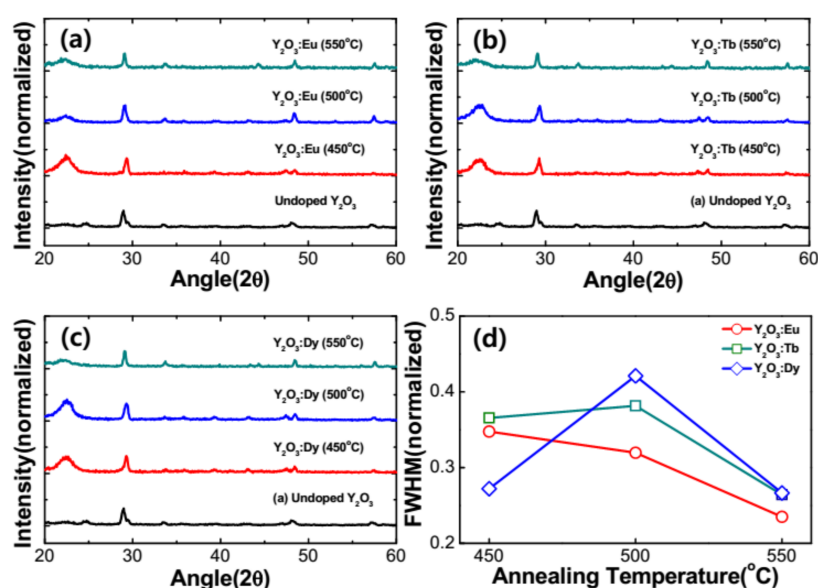


Figure 2. XRD patterns of the RE-doped Y_2O_3 for different annealing temperatures at 450, 500, 550 °C. (a) 0.05 mM of Eu^{3+} -doped Y_2O_3 core, (b) 0.05 mM of Tb^{3+} -doped Y_2O_3 core and (c) 0.05 mM of Dy^{3+} -doped Y_2O_3 core, and (d) FWHM of RE (Eu, Tb and Dy)-doped Y_2O_3 at 450, 500, 550 °C.

Table 1. Structural parameters of the RE^{3+} -doped nanophosphors.

Sample	Annealing Temperature (°C)	Crystallite Size, D (nm)		Reference
		Debye–Scherrer	Hall–Williamsons	
$\text{Y}_2\text{O}_3:\text{Eu}$	450	23		Present work
	500	25		
	550	34		
$\text{Y}_2\text{O}_3:\text{Tb}$	450	22		
	500	21		
	550	31		
$\text{Y}_2\text{O}_3:\text{Dy}$	450	30		
	500	19		
	550	30		
$\text{Y}_2\text{O}_3:\text{Tb}$	500		15	[17]
$\text{Y}_2\text{O}_3:\text{Eu}$	500		18	[18]

The morphology of the synthesized undoped and RE^{3+} -doped nanophosphors was analyzed by scanning electron microscope (SEM) and transmission electron microscope

(TEM) techniques. Figure 3a–d show the SEM images of undoped Y_2O_3 and $\text{RE}^{3+}\text{-Y}_2\text{O}_3$ (RE = Eu, Tb, and Dy) nanophosphors. It is noticed that the resultant nanoparticles are in a spherical shape and uniform with an average size of approximately 100–150 nm. The inset of Figure 3a–d shows the TEM images of the undoped Y_2O_3 and $\text{Y}_2\text{O}_3\text{:RE}^{3+}$ (RE = Eu, Tb, and Dy) nanophosphors. The change in mass ratio of the YCl_3 raw material and Y_2O_3 core can control the shell layer thickness deposited around the core. TEM images confirmed the thickness of the core–shell nanoparticles. It is found that the surface of Y_2O_3 nanoparticles have irregular shell structures. It is worth mentioning that the exact thickness of the shell layer is difficult to determine from the TEM images due to slight contrast at core–shell interface.

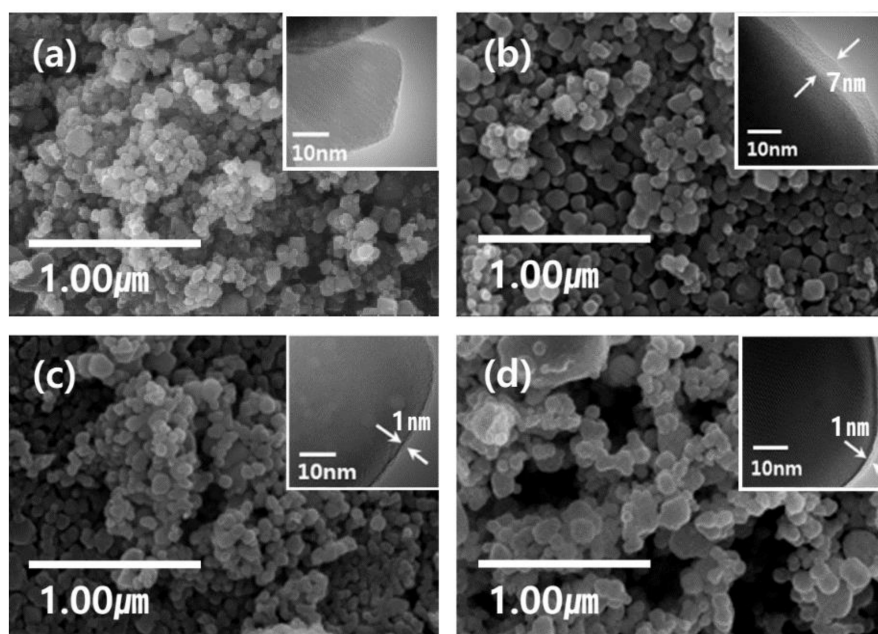


Figure 3. SEM and TEM images (a) Y_2O_3 NP core sintered at 550°C for 3 h, (b) Eu-doped Y_2O_3 NP active core with a passive Y_2O_3 shell, (c) Tb-doped Y_2O_3 NP active core with a passive Y_2O_3 shell, (d) Dy-doped Y_2O_3 NP active core with a passive Y_2O_3 shell. The inset TEM images show the coating thickness of each sample.

Figure 4a shows the luminescence spectra of 0.05 mMol% $\text{Eu}^{3+}\text{:Y}_2\text{O}_3$ nanophosphor, obtained under 254 nm excitation, respectively. As can be seen from the figure, the luminescence spectra exhibited emission lying between 580 nm and 700 nm originating from the $^5\text{D}_0 \rightarrow ^7\text{F}_j$ ($j = 0\text{--}3$) transitions of the Eu^{3+} ion. Among the emission peaks, the strongest peak at 611 nm and a less intense peak at 630 nm attributed to the $^5\text{D}_0 \rightarrow ^7\text{F}_2$ electric-dipole hypersensitive transition of Eu^{3+} ion in the yttrium oxide host and its intensity is sensitive to the environment, while the weak emission peaked at 580 nm corresponds to the $^5\text{D}_0 \rightarrow ^7\text{F}_0$ transition. The weak emission in the region 587–600 nm corresponds to the $^5\text{D}_0 \rightarrow ^7\text{F}_1$ magnetic-dipole transition of Eu^{3+} ion. Generally, the emission band at 611 nm can show strong emission when Eu^{3+} is located at a lower symmetry (without an inversion center), whereas the emission of magnetic dipole transition at 590 nm is stronger when Eu^{3+} is located at a higher symmetry (with an inversion center). From the emission spectrum of Eu^{3+} ion, it is clearly indicated that the Eu^{3+} ions are situated at lower symmetry as the emission at 611 nm corresponding to the $^5\text{D}_0 \rightarrow ^7\text{F}_2$ transition is dominant. From the emission spectrum in Figure 4a, it is confirmed that Eu^{3+} ions are preferably situated at crystallographic site without inversion center (C_2) [19]. Figure 4b depicts the emission spectrum of $\text{Y}_2\text{O}_3\text{:0.05 mMol% Tb}^{3+}$, obtained under 280 nm excitation. The luminescence spectrum exhibits its strongest peaks at around 545 nm (green emission), and a weak peak centered at 583 nm attributed to the $^5\text{D}_4 \rightarrow ^7\text{F}_5$, and $^5\text{D}_4 \rightarrow ^7\text{F}_4$ transitions of

Tb³⁺ ion, respectively. Figure 4c displays the luminescence spectrum of the Dy³⁺-doped Y₂O₃ nanophosphors, obtained under an excitation wavelength of 350 nm. As can be seen from the emission spectrum of the Tb³⁺ ion, it is observed that the Dy³⁺ ion exhibits strong blue emission at around 472 nm attributed to the ⁴F_{9/2} → ⁶H_{15/2} transition of the Dy³⁺ ion (magnetic-dipole transition, insensitive to the local environment).

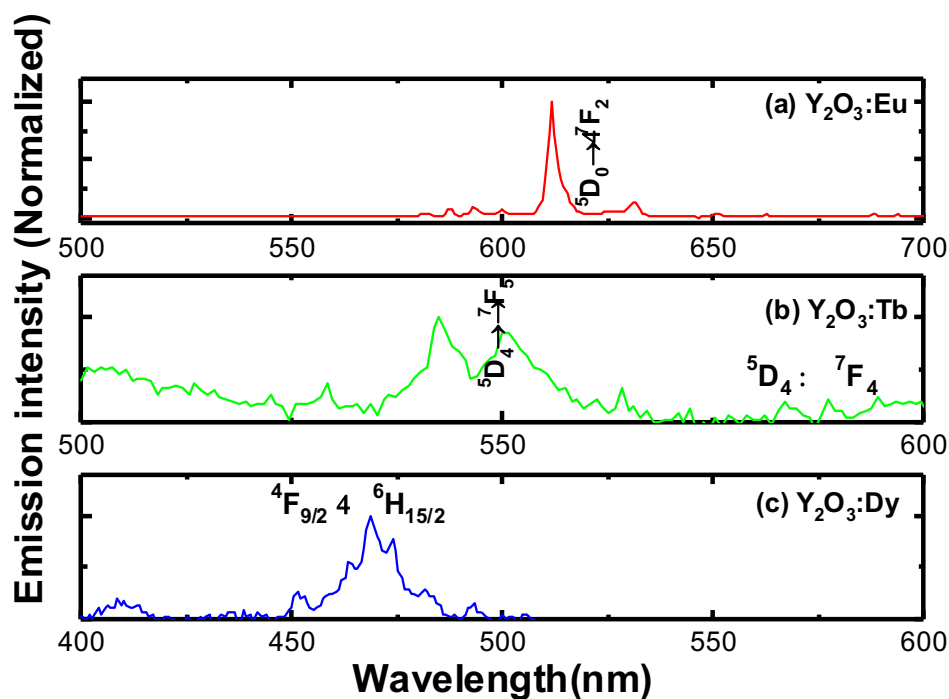


Figure 4. Luminescence spectra of (a) 0.05 m Mol% Eu:Y₂O₃, (b) 0.05 m Mol% Tb:Y₂O₃, and (c) 0.05 m Mol% Dy:Y₂O₃ nanophosphors.

Based on the reported literature, it can be noticed that the RE³⁺ ion's luminescence is often improved by thermal treatment. In this study, the effect of the annealing temperature on the luminescence properties of nanophosphors was investigated. The RE³⁺-doped Y₂O₃ nanophosphors were annealed in the temperature range from 450 to 550 °C. Figure 5a shows the variation of the luminescence intensity of RE³⁺-doped Y₂O₃ nanophosphor in the dependence of annealing temperature. It was found that the emission intensity of Eu³⁺ ion increased with the increase in annealing temperature due to the improvement of crystallite size in the Y₂O₃ nanophosphors. The same trend was observed in Eu³⁺-doped Y₂O₃ nanoparticles synthesized by the other methods [11,18,20]. The variation of emission intensity in Tb³⁺-doped Y₂O₃ nanophosphors in the dependence of annealing temperature as shown in Figure 5a. The emission intensity of Tb³⁺ ions at the green region increased with the increase in annealing temperature which changed from 450 to 550 °C. The trend of emission intensity in the dependence of annealing temperature could be due to a reduction in surface OH groups and the improvement of crystallite size of the nanophosphors. Figure 5a shows the variation of emission intensity for different annealing temperatures in Dy³⁺-doped Y₂O₃ nanophosphors. No considerable variation in the emission intensity for the annealed Dy³⁺-doped nanophosphors. This indicates that the Dy³⁺ environment was not changed with annealing temperature.

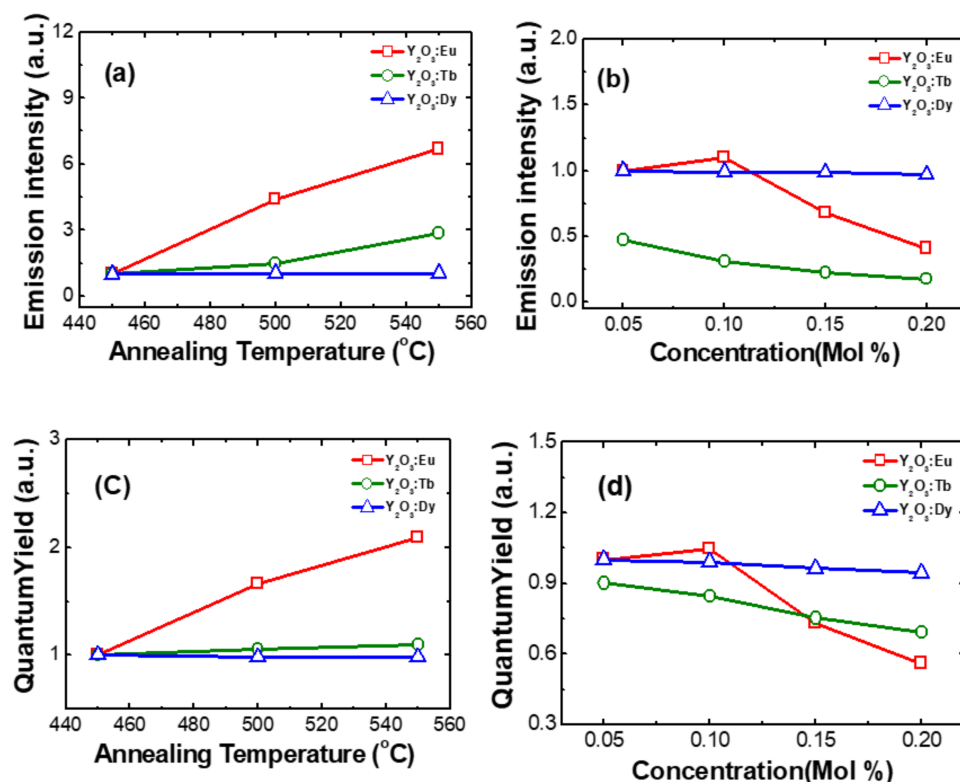


Figure 5. (a) Variation of emission intensity with annealing temperature at 450, 500, 550 °C, (b) Variation of emission intensity with concentration at 0.05, 0.10, 0.15, 0.20 mMol%, (c) Variation of quantum yield with annealing temperature at 450, 500, 550 °C, and (d) Variation of quantum yield with concentration at 0.05, 0.10, 0.15, 0.20 mMol% in RE³⁺ (Eu, Tb, Dy)-doped nanophosphors.

The effect of Eu³⁺ ions concentration on luminescence properties in Y₂O₃ nanophosphors was investigated as shown in Figure 5b. The emission intensity of Eu³⁺-doped Y₂O₃ nanophosphors (at 611 nm) increased with the increase in Eu³⁺ concentration up to 0.1 mol% and then decreased for further increase in Eu³⁺ ion concentration. The optimum Eu doping concentration in Y₂O₃ nanophosphor was obtained as 0.1 mol%. The enhanced intensity can be attributed to the increased luminescence active centers, while it decreased for higher Eu doping due to energy transfer through the cross-relaxation mechanism: Eu³⁺ (⁵D₁) + Eu³⁺ (⁷F₀) → Eu³⁺ (⁵D₀) + Eu³⁺ (⁷F₁) [21]. Figure 5b shows the emission intensity of Tb³⁺-doped Y₂O₃ nanophosphor with varying concentration. As the concentration of Tb³⁺ increases, the luminescence intensity decreases in the synthesized nanophosphors. The trend of the Tb³⁺ ion emission intensity with respect to concentration due to the energy transfer through the cross-relaxation mechanism between neighboring Tb³⁺ ions: Tb³⁺ (⁵D₃) + Tb³⁺ (⁷F₆) → Tb³⁺ (⁵D₄) + Tb³⁺ (⁷F₀). The intensity of the Dy³⁺ characteristic transition was not changed considerably with respect to the Dy³⁺ concentration varied from 0.05 to 0.2 mol% as shown in Figure 5b.

The photoluminescence QY of RE³⁺-doped Y₂O₃ nanophosphors was analyzed for different annealing temperatures and RE³⁺ ion concentrations as shown in Figure 5c,d. In the case of Eu³⁺-doped Y₂O₃ nanophosphor, the QY increased when the annealing temperature varied from 450 to 550 °C. When we consider the concentration, QY initially increases up to 0.1 mol% and then decreases after further increase in concentration up to 0.2 mol%. This illustrates the importance of considering different concentrations. The QY of Y₂O₃:Tb³⁺ and Y₂O₃:Dy³⁺ nanophosphors showed slight variation when annealing temperature and concentration varied as illustrated in Figure 5c,d.

Figure 6a–c show the diffraction patterns of the as-prepared and RE³⁺-doped Y₂O₃ core with Y₂O₃ passive shell nanophosphors annealed in the temperature range from 450 to 550 °C. From the figure, it is clear that the similar XRD patterns are observed for

RE³⁺-doped Y₂O₃ core with Y₂O₃ passive shell nanophosphors when compared to the core nanoparticles. This indicates that the RE³⁺-doped nanoparticles exhibited a Y₂O₃ cubic crystal structure even with RE doping, a core–shell structure and annealed at different temperatures. Figure 6d presents the variation of FWHM with respect to the annealing temperature for the RE³⁺-doped Y₂O₃ core with Y₂O₃ passive shell. It is observed that the FWHM of RE³⁺-doped Y₂O₃ core with Y₂O₃ passive shell were analogous to the RE³⁺-doped Y₂O₃ core nanoparticles. The crystallite size of the nanophosphors was also improved with the core–shell nanostructure.

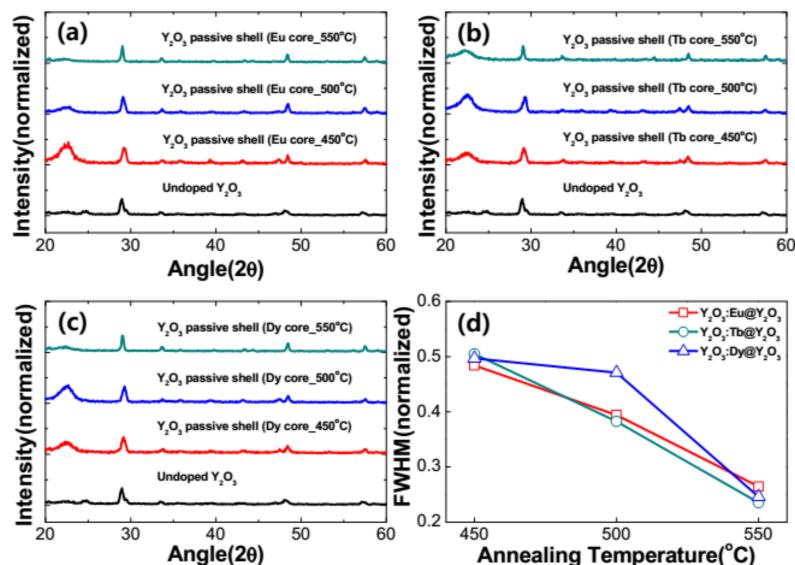


Figure 6. XRD patterns of the RE-doped Y₂O₃ core coated with Y₂O₃ passive shell via different annealing temperatures at 450, 500, 550 °C. (a) An amount of 0.05 mM of Eu³⁺-doped Y₂O₃ core with a Y₂O₃ passive shell, (b) 0.05 mM of Tb³⁺-doped Y₂O₃ core with a Y₂O₃ passive shell and (c) 0.05 mM of Dy³⁺-doped Y₂O₃ core with a Y₂O₃ passive shell, and (d) FWHM of RE (Eu, Tb and Dy)-doped Y₂O₃ core with a Y₂O₃ passive shell at 450, 500, 550 °C.

The 0.10 mMol% of Eu³⁺, 0.05 mMol% of Tb³⁺, and 0.05 mMol% of Dy³⁺-doped Y₂O₃ samples were chosen to compare the luminescence properties of RE³⁺-doped Y₂O₃ cores and RE³⁺-doped Y₂O₃ cores with Y₂O₃ passive shells as they exhibited the optimum luminescence intensity. Figure 7 definitively shows that the core–shell phosphors revealed a higher peak intensity as compared to the core nanoparticles due to increase in distance between surface quenching sites and RE³⁺ active ions. After the passive shell coating, the QY was also measured for the RE³⁺-doped core–shell nanoparticles along with RE³⁺-doped core nanoparticles (see Figure 8). Variation in emission intensity (Figures 4 and 5a,b) is qualitative. In order to perform quantitative measurement, the photoluminescence quantum yield (QY) (based on integrated sphere) was carried out for the synthesized RE³⁺-doped nanophosphors with a core–shell structure. The photoluminescence QY is defined as the ratio of number of photons emitted to the number of photons absorbed. All of the reflected and emitted light can be collected where the concern regarding the angular dependence of the photoluminescence emission is no longer needed by implementing integrating sphere into photoluminescence QY measurements. Mello et al. [22] developed an equation for the determination of absolute photoluminescence QY as shown below,

$$\Phi_{PL} = \frac{E_{in}(\lambda) - (1 - \alpha)E_{out}(\lambda)}{X_{empty}(\lambda)\alpha}$$

with

$$\alpha = \frac{X_{out}(\lambda) - X_{in}(\lambda)}{X_{out}(\lambda)}$$

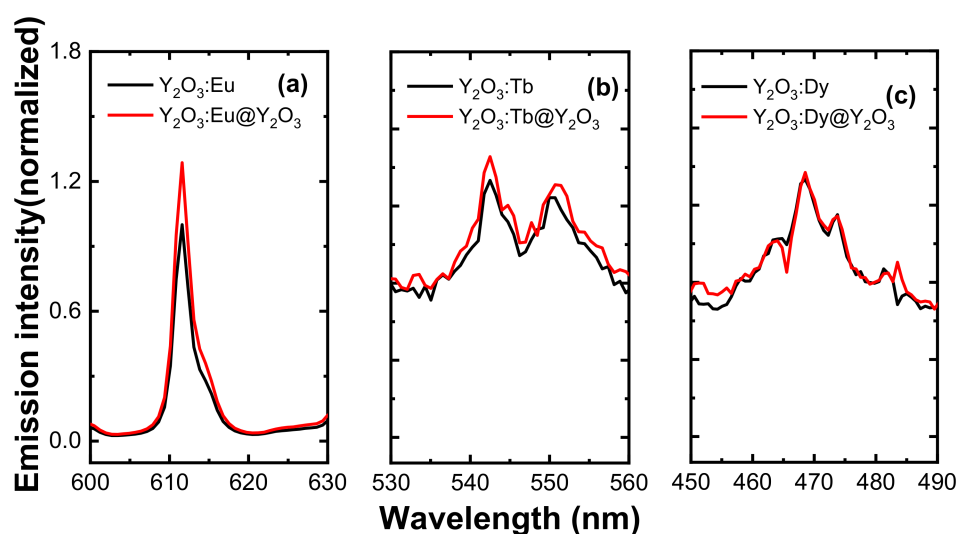


Figure 7. Relative luminescence spectra of the RE-doped Y₂O₃ core and Y₂O₃ passive shell-coated Y₂O₃:RE core. (a) Relative luminescence spectra of 0.10 mM of Eu³⁺-doped Y₂O₃ core and Y₂O₃:Eu@Y₂O₃, (b) relative luminescence spectra of 0.05 mM of Tb³⁺-doped Y₂O₃ core and Y₂O₃:Tb@Y₂O₃, (c) relative luminescence spectra of 0.05 mM of Dy³⁺-doped Y₂O₃ core and Y₂O₃:Dy@Y₂O₃. All the core samples were annealed at 550 °C for 3 h and passive shells were annealed at 750 °C for 3 h.

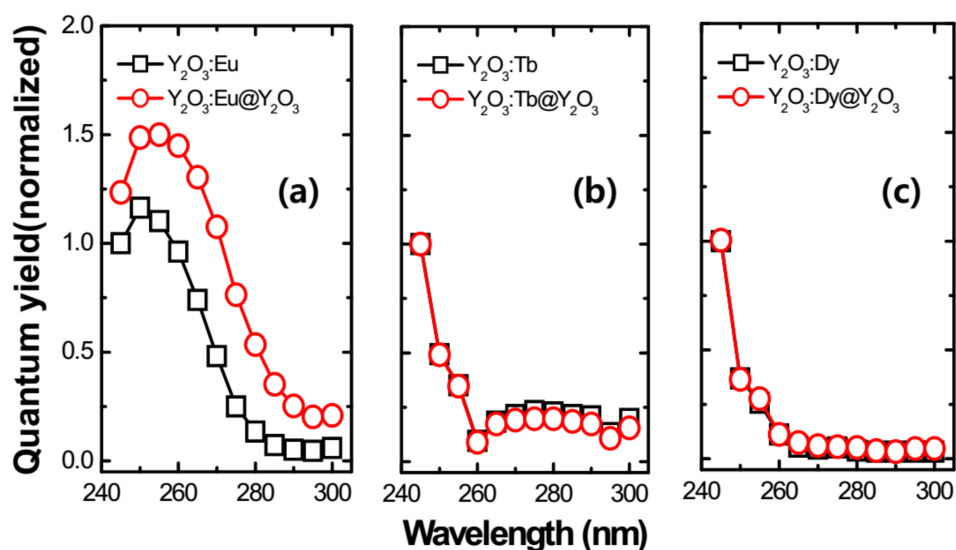


Figure 8. Relative quantum yield spectra of the RE-doped Y₂O₃ core and Y₂O₃ passive shell-coated Y₂O₃:RE core. (a) Relative quantum yield of 0.10 mM of Eu³⁺-doped Y₂O₃ core and Y₂O₃:Eu@Y₂O₃, (b) relative quantum yield of 0.05 mM of Tb³⁺-doped Y₂O₃ core and Y₂O₃:Tb@Y₂O₃, (c) relative quantum yield of 0.05 mM of Dy³⁺-doped Y₂O₃ core and Y₂O₃:Dy@Y₂O₃. All the core samples were annealed at 550 °C for 3 h and passive shells were annealed at 750 °C for 3 h.

In the above equations, $E_{in}(\lambda)$ and $E_{out}(\lambda)$ are the integrated luminescence as a result of direct excitation and secondary excitation of the sample, respectively. The latter emission is due to reflected excitation light from sphere walls hitting the sample. $X_{empty}(\lambda)$ is the integrated excitation profile with the empty sphere. α is the sample absorbance. The product of the photoluminescence QY and absorption coefficient reveals the brightness of a photoluminescent nanoparticle of the material. The absorption is an intrinsic characteristic of the material, while photoluminescence QY depends on the architecture of the nanoparticle and its immediate environment. It is widely accepted that core/shell

engineering of RE-doped nanophosphors allows researchers to substantially improve the photoluminescence QY of the nanophosphors and subsequently their brightness, by means of an optically undoped passive layer. Safeguarding the emission intensity by a passive layer is attained by spatially separating the optically active core from the structural surface defects at the core interface. It can be seen that the QY increased significantly after shell coating in the $\text{Y}_2\text{O}_3:\text{Eu}^{3+}$ nanophosphor. No considerable variation was noticed in the case of $\text{Y}_2\text{O}_3:\text{Tb}^{3+}$ and $\text{Y}_2\text{O}_3:\text{Dy}^{3+}$ nanophosphors.

4. Conclusions

In this work, the luminescence properties of RE^{3+} -doped Y_2O_3 core and core-shell nanoparticles synthesized by the molten salt synthesis and sol-gel processes were investigated in the dependence of annealing temperature and active ion concentration. The morphology studies of the Y_2O_3 core and core-shell nanoparticles confirmed the nanoparticle size as approximately 100–150 nm in diameter with shell layer thickness up to 8 nm. The diffraction patterns of as-prepared, RE-doped core, and core-shell nanoparticles annealed at different temperatures showed a cubic Y_2O_3 crystal structure (JCPDS 41-1105). The optimum active ion concentration based on luminescence intensity was found to be 0.10 mMol%, 0.05 mMol%, and 0.05 mMol% for Eu^{3+} -, Tb^{3+} -, and Dy^{3+} -doped nanophosphors, respectively. The luminescence intensity and quantum yield of RE-doped core-shell nanoparticles were compared with the Y_2O_3 core nanoparticles. The luminescence intensity and quantum yield of Eu^{3+} -doped core nanophosphors enhanced after coating with the Y_2O_3 passive shell layer. No considerable variation was noticed in case of Tb^{3+} - and Dy^{3+} -doped Y_2O_3 nanophosphors.

Author Contributions: Conceptualization, W.-B.I. and J.-H.C.; methodology, J.-Y.H. and K.-H.K.; formal analysis, K.L. and J.-P.K.; investigation, J.-P.K. and J.-H.C.; writing—original draft preparation, J.-Y.H. and K.-H.K.; writing—review and editing, K.L., W.-B.I. and J.-H.C. All authors have read and agreed to the published version of the manuscript.

Funding: This work was supported by the Materials and Components Technology Development Program of MOTIE/KEIT, 20011325 (High refractive optical glass for GMP).

Data Availability Statement: Not applicable.

Conflicts of Interest: The authors declare no conflict of interest.

References

1. Ronda, C.R. Phosphors for lamps and displays. *J. Alloys Compd.* **1995**, *225*, 534–538. [[CrossRef](#)]
2. Song, H.W.; Chen, B.J.; Peng, H.S.; Zhang, J.S. Light-induced change of charge transfer band in nanocrystalline $\text{Y}_2\text{O}_3:\text{Eu}^{3+}$. *Appl. Phys. Lett.* **2002**, *81*, 1776–1778. [[CrossRef](#)]
3. Wegh, R.T.; Donker, H.; Oskam, K.D.; Meijerink, A. Visible quantum cutting in $\text{LiGdF}_4:\text{Eu}^{3+}$ through downconversion. *Science* **1999**, *283*, 663–666. [[CrossRef](#)] [[PubMed](#)]
4. Mao, Y.; Tran, T.; Guo, X.; Huang, J.Y.; Shih, C.K.; Wang, K.L.; Chang, J.P. Luminescence of nanocrystalline erbium-doped yttria. *Adv. Funct. Mater.* **2009**, *19*, 748–754. [[CrossRef](#)]
5. Singh, L.R.; Ningthoujam, R.S.; Sudarsan, V.; Srivastava, I.; Singh, S.D.; Dey, G.K.; Kulshreshtha, S.K. Luminescence study on Eu^{3+} doped Y_2O_3 nanoparticles: Particle size, concentration and core-shell formation effects. *Nanotechnology* **2008**, *19*, 055201–055210. [[CrossRef](#)] [[PubMed](#)]
6. Kodaira, C.A.; Stefani, R.; Maia, A.S.; Felinto, M.C.F.C.; Brito, H.F. Optical investigation of $\text{Y}_2\text{O}_3:\text{Sm}^{3+}$ nanophosphor prepared by combustion and Pechini methods. *J. Lumin.* **2007**, *127*, 616–622. [[CrossRef](#)]
7. Xu, Z.X.; Hong, Z.; Zhao, Q.; Peng, L.; Zhang, P. Preparation and Luminescence Properties of $\text{Y}_2\text{O}_3:\text{Eu}^{3+}$ Nanorods via Post Annealing Process. *J. Rare Earths* **2006**, *24*, 111–114.
8. Yan, Y.; Faber, A.J.; de Waal, H. Luminescence quenching by OH groups in highly Er-doped phosphate glasses. *J. Non Cryst. Solids* **1995**, *181*, 283–290. [[CrossRef](#)]
9. Parchur, A.K.; Prasad, A.I.; Ansari, A.A.; Rai, S.B.; Ningthoujam, R.S. Luminescence properties of Tb^{3+} -doped CaMoO_4 nanoparticles: Annealing effect, polar medium dispersible, polymer film and core-shell formation. *Dalton Trans.* **2012**, *41*, 11032–11045. [[CrossRef](#)]
10. Dorman, J.A.; Choi, J.H.; Kuzmanich, G.; Chang, J.P. Elucidating the Effects of a Rare-Earth Oxide Shell on the Luminescence Dynamics of $\text{Er}^{3+}:\text{Y}_2\text{O}_3$ Nanoparticles. *J. Phys. Chem. C* **2012**, *116*, 10333–10340. [[CrossRef](#)]

11. Hari Krishna, R.; Nagabhushana, B.M.; Nagabhushana, H.; Suriya Murthy, N.; Sharma, S.C.; Shivakumara, C.; Chakradhar, R.P.S.J. Effect of Calcination Temperature on Structural, Photoluminescence, and Thermoluminescence Properties of $Y_2O_3:Eu^{3+}$ Nanophosphor. *J. Phys. Chem. C* **2013**, *117*, 1915–1924. [[CrossRef](#)]
12. Liu, Z.; Yu, L.; Wang, Q.; Tao, Y.; Yang, H. Effect of Eu,Tb codoping on the luminescent properties of Y_2O_3 nanorods. *J. Lumin.* **2011**, *131*, 12–16. [[CrossRef](#)]
13. Park, J.-H.; Back, N.G.; Hong, K.-S.; Kim, C.-S.; Yoo, D.-H.; Kwak, M.G.; Han, J.-I.; Sung, J.-H.; Moon, B.K.; Seo, H.-J. Annealing effect on photoluminescence intensity of Eu-doped Y_2O_3 nanocrystals. *J. Korean Phys. Soc.* **2005**, *47*, S368–S371.
14. Li, R.; Zi, W.; Li, L.; Zhang, J.; Zou, L.; Gan, S. Monodisperse and hollow structured $Y_2O_3:Ln^{3+}$ ($Ln = Eu, Dy, Er, Tm$) nanospheres: A facile synthesis and multicolor-tunable luminescence properties. *J. Alloys Compd.* **2014**, *617*, 498–504. [[CrossRef](#)]
15. Atabaev, T.S.; Hwang, Y.-H.; Kim, H.-K. Color-tunable properties of Eu^{3+} - and Dy^{3+} -codoped Y_2O_3 phosphor particles. *Nanoscale Res. Lett.* **2012**, *7*, 556. [[CrossRef](#)] [[PubMed](#)]
16. Khachatourian, A.M.; Golestani-Fard, F.; Sarpoolaky, H.; Vogt, C.; Vasileva, E.; Mensi, M.; Popov, S.; Toprak, M.S. Microwave synthesis of $Y_2O_3:Eu^{3+}$ nanophosphors: A study on the influence of dopant concentration and calcination temperature on structural and photoluminescence properties. *J. Lumin.* **2016**, *169*, 1–8. [[CrossRef](#)]
17. Som, S.; Sharma, S.K. Eu^{3+}/Tb^{3+} -codoped Y_2O_3 nanophosphors: Rietveld refinement, bandgap and photoluminescence optimization. *J. Phys. D Appl. Phys.* **2012**, *45*, 415102. [[CrossRef](#)]
18. Boukerika, A.; Guerbous, L. Annealing effects on structural and luminescence properties of red Eu^{3+} -doped Y_2O_3 nanophosphors prepared by sol–gel method. *J. Lumin.* **2014**, *145*, 148–153. [[CrossRef](#)]
19. Wang, L.; Jia, H.; Yu, X.; Zhang, Y.; Du, P.; Xi, Z.; Jin, D. Optimization of the Photoluminescence Properties of Electrodeposited $Y_2O_3:Eu^{3+}$ Thin-Film Phosphors. *Electrochem. Solid State Lett.* **2009**, *12*, E20–E22. [[CrossRef](#)]
20. Xiao, Y.; Wu, D.; Jiang, Y.; Liu, N.; Liu, J.; Jiang, K. Nano-sized $Y_2O_3:Eu^{3+}$ hollow spheres with enhanced photoluminescence properties. *J. Alloys Compd.* **2011**, *509*, 5755–5760. [[CrossRef](#)]
21. Mueller, R.; Madler, L.; Pratsinis, S.E. Nanoparticle synthesis at high production rates by flame spray pyrolysis. *Chem. Eng. Sci.* **2003**, *58*, 1969–1976. [[CrossRef](#)]
22. De Mello, J.C.; Wittmann, H.F.; Friend, R.H. An improved experimental determination of external photoluminescence quantum efficiency. *Adv. Mater.* **1997**, *9*, 230–232. [[CrossRef](#)]